Application of Metagenomic Long-Read Sequencing for the Diagnosis of Herpetic Uveitis

Yoshito Koyanagi,[1] Ai Fujita Sajiki,[1] Kenya Yuki,[1] Hiroaki Ushida,[1] Kenichi Kawano,[1,2] Kosuke Fujita,[1] Hideyuki Shimizu,[1] Daishi Okuda,[1] Mitsuki Kosaka,[1] Kazuhisa Yamada,[1] Ayana Suzumura,[1] Shu Kachi,[3] Hiroki Kaneko,[1] Hiroyuki Komatsu,[4] Yoshihiko Usui,[4] Hiroshi Goto,[4] and Koji M. Nishiguchi[1]

[1]Department of Ophthalmology, Nagoya University Graduate School of Medicine, Nagoya, Japan
[2]Department of Ophthalmology, Yokkaichi Municipal Hospital, Yokkaichi, Japan
[3]Shohzankai Medical Foundation, Miyake Eye Hospital, Nagoya, Japan
[4]Department of Ophthalmology, Tokyo Medical University, Tokyo, Japan

Correspondence: Kenya Yuki, Department of Ophthalmology, Nagoya University Graduate School of Medicine, 65 Tsurumai-cho, Showa-ku, Nagoya 466-8550, Japan; yuki.kenya.z9@f.mail.nagoya-u.ac.jp.

YK and AFS are joint first authors.

Received: November 2, 2024
Accepted: March 11, 2025
Published: April 17, 2025

Citation: Koyanagi Y, Sajiki AF, Yuki K, et al. Application of metagenomic long-read sequencing for the diagnosis of herpetic uveitis. *Invest Ophthalmol Vis Sci.* 2025;66(4):50. https://doi.org/10.1167/iovs.66.4.50

Purpose. To investigate the sensitivity and specificity of herpes virus detection by nanopore metagenomic analysis (NMA) compared with multiplex polymerase chain reaction (mPCR)-positive and -negative controls.

Methods. This study included 43 patients with uveitis who had been screened for intraocular herpes virus infection using mPCR from aqueous humor samples. Aqueous humor samples stored after mPCR were subjected to whole-genome amplification, long-read sequencing, and analysis of the phylogenetic microorganism composition using a Flongle flow cell on the Oxford Nanopore MinION platform. For samples that tested positive with mPCR and negative with the Flongle flow cell, additional long-read sequencing was performed using a MinION flow cell, which enabled acquisition of more sequence data. The sensitivity and specificity of herpes virus detection by NMA were compared with the mPCR-positive and -negative controls.

Results. NMA using a Flongle flow cell detected the pathogenic virus in 60.0% of those who tested positive by mPCR (12/20). Further analysis using the MinION flow cell successfully identified viral DNA fragments in three out of the eight initially undetected samples, yielding a collective sensitivity of 75.0% (15/20). All of the virus detected with the long-read sequencing were identical to those diagnosed by mPCR testing, and none of the samples that tested negative by mPCR revealed herpes viral DNA with the use of long-read sequencing.

Conclusions. For the detection of etiologic herpes virus DNA fragments, NMA revealed a reasonable sensitivity and high specificity. Our study highlights the potential of nanopore sequencing to facilitate further advances in uveitis diagnosis.

Keywords: herpetic uveitis, metagenomic analysis, multiplex polymerase chain reaction, nanopore DNA sequencing, ocular infectious diseases

In the field of ophthalmology, multiplex polymerase chain reaction (mPCR) testing is commonly used to detect major etiologic microorganisms in intraocular fluid and corneal specimens. This technique has demonstrated high concordance rates with conventional quantitative PCR (qPCR) and has contributed to improvement of the diagnosis of ocular infectious diseases, particularly herpes virus infections.[1–3] However, despite widespread use of this technique in Japan, infectious uveitis accounts for only 16% of all uveitis cases, and the cause of inflammation remains unidentified and undiagnosed in 37.3% of all cases.[4] This value is comparable to the frequency of undiagnosed cases in other developed countries, which ranges from 31.8% to 44.4%.[5–8] Therefore, it is conceivable that unidentified infectious pathogens are responsible for the disease in certain cases. Indeed, recently, adenovirus has been newly ascertained as a novel cause of a retinal inflammatory disease.[9,10] Furthermore, improving the ocular infection diagnostic rate is a topic of great clinical importance, as most infections can be treated with antibiotics and antivirals and the treatment strategy is fundamentally different from that of noninfectious diseases, which primarily aims to suppress inflammation.

Recently, metagenomic analysis, an approach to sequence the whole combination of DNA and/or RNA of microorganisms and host purified directly from specimens comprehensively, bypassing the conventional culturing process, is being widely explored in the research of infectious diseases, including influenza virus, viral meningoencephalitis, and COVID-19 infection.[11–13] Unlike conventional mPCR, which is a current gold standard method for specifically detecting the genome of predefined pathogens, metagenomic analysis is hypothesis free, as it extracts and analyzes genetic information from all microorganisms present without prior knowledge. Additionally, metagenomic analysis

enables detailed species identification and functional annotation analysis, providing detailed insights into the microbial community.

The MinION (Oxford Nanopore Technologies, Oxford, UK), a portable, mouse-sized, artificial intelligence–equipped long-read sequencer, has gained attention as a new sequencing platform.[14–16] Genomic analysis, which combines metagenomic analysis using nanopores and qPCR, has been compared to culture, the golden standard for clinical diagnosis, and has shown almost 100% sensitivity and specificity for detecting bacterial lower respiratory tract infections.[17] Nanopore whole-genome sequencing also demonstrated 100% agreement with culture for endophthalmitis, representing the highest concordance compared to 16S nanopore and Illumina whole-genome sequencing.[18] These findings suggest that metagenomic analysis could become the new standard for infectious disease diagnosis.

Although there have been several reports on the application of nanopore sequencing to ophthalmic infectious diseases, especially bacterial- and fungi-related endophthalmitis,[18–22] no study has been conducted in the field of ophthalmology applying nanopore long-read sequencing to viral infections and investigating sensitivity and specificity compared with mPCR-positive and -negative controls. Herein, we aimed to apply this compact nanopore metagenomic sequencer to diagnose herpetic uveitis. We performed long-read sequencing of samples obtained from the aqueous humor of patients pre-assessed using mPCR and attempted to detect the etiologic herpes virus by comprehensive metagenomic analysis.

Methods

Study Design and Participants

This was a retrospective cross-sectional study. Participants were recruited from Nagoya University Hospital and Tokyo Medical University Hospital, and clinical information was retrospectively obtained from medical records.

Table 1. Clinical Characteristics of Patients With mPCR-Positive Uveitis

	mPCR-Positive Controls		
	NMA-Positive Controls	**NMA-Negative Controls**	***P***
Age (y), mean ± SD	59.1 ± 14.6	61.0 ± 8.7	0.97
Sex, *n* (%)			
Male	8 (53.3)	3 (60.0)	1.0
Female	7 (46.6)	2 (40.0)	
Types of herpes viruses detected in the aqueous humor, *n* (%)			
HSV1	0 (0.0)	1 (20.0)	0.25
HSV2	0 (0.0)	1 (20.0)	0.25
VZV	7 (46.7)	1 (20.0)	0.6
EBV	1 (6.7)	0 (0.0)	1.0
CMV	7 (46.7)	2 (40.0)	1.0
Types of uveitis, *n* (%)			
Panuveitis	7 (46.7)	2 (40.0)	1.0
Anterior	7 (46.7)	3 (60.0)	1.0
Intermediate	0 (0.0)	0 (0.0)	1.0
Posterior	0 (0.0)	0 (0.0)	1.0
Intraocular lens, *n* (%)	4 (26.7)	2 (40.0)	0.61
Steroid eye drops, *n* (%)	3 (20.0)	2 (40.0)	0.56
Immunodeficiency details, *n* (%)			
Diabetes mellitus	2 (13.3)	1 (20.0)	1.0
Oral corticosteroids	1 (6.7)	1 (20.0)	0.45
Lymphoid neoplasm	3 (20.0)	0 (0.0)	1.0
Post-transplantation status	1 (6.7)	1 (20.0)	0.45
Human immunodeficiency virus infection	1 (6.7)	0 (0.0)	1.0
History of antiviral treatment, *n* (%)	12 (80.0)	5 (100)	0.54
Type of antiviral, *n* (%)			
Acyclovir	2 (13.3)	1 (20.0)	1.0
Ganciclovir	8 (53.3)	2 (40.0)	1.0
Valaciclovir	4 (26.7)	3 (60.0)	0.29
Valganciclovir	5 (33.3)	1 (20.0)	1.0
Foscarnet	4 (26.7)	0 (0.0)	0.53
Differences in clinical parameters at pre- and posttreatment			
Median BCVA (logMAR) decrease	0.17	0.08	0.97
Median IOP (mm Hg/NCT) decrease	−3.0	−1.0	0.19
Improvement of clinical parameters at pre- and posttreatment, *n* (%)			
Cells in the anterior chamber	8 (53.3)	3 (60.0)	1.0
Cells in the vitreous	7 (46.7)	3 (60.0)	1.0
Vitreous opacity	6 (40.0)	1 (20.0)	0.61
Macular edema	6 (40.0)	1 (20.0)	0.61
Response to antiviral treatment, *n* (%)	7 (53.8)	2 (40.0)	0.62
Mean final BCVA (logMAR)	0.66	0.12	0.15

NCT, non-contact tonometry. To analyze between-group differences, the Kruskal–Wallis test or Fisher's exact test was used. $P < 0.05$ is considered statistically significant.

Investigative Ophthalmology & Visual Science

Table 2. Clinical Characteristics of Patients and Summary of the Nanopore Metagenomic Analysis for mPCR-Positive Uveitis

				mPCR		NMA		
ID	Gender	Age (y)	Disease	Type of Herpes Virus	DNA Copy Number	Flongle Flow Cell	MinION Flow Cell	Pavian Plot
P5	M	61	CMV retinitis	CMV	Unmeasured	Positive	—	Fig. 1
P6	F	73	CMV retinitis	CMV	Unmeasured	Positive	—	Fig. S1
P7	F	63	CMV retinitis	CMV	Unmeasured	ND	ND	Fig. S1
P8	M	62	Herpetic iridocyclitis	CMV	Unmeasured	ND	ND	Fig. S1
P9	M	66	Herpetic iridocyclitis	CMV	Unmeasured	ND	Positive	Figs. S1, S4
P10	M	59	CMV retinitis	CMV	9.6×10^5	Positive	—	Fig. S1
P11	M	73	CMV retinitis	CMV	5.8×10^2	ND	Positive	Fig. S2
P12	F	46	CMV retinitis	CMV	Unmeasured	ND	Positive	Figs. S1, S4
P13	F	64	CMV retinitis	CMV	4.2×10^3	Positive	—	Fig. S1
P18	M	74	Herpetic iridocyclitis	HSV1	7.1×10^3	ND	ND	Fig. S1
P19	F	53	Herpetic iridocyclitis	HSV2	7.3×10^3	ND	ND	Fig. S1
P20	M	64	Herpetic iridocyclitis	VZV	7.3×10^5	Positive	—	Fig. S1
P21	M	53	ARN	VZV	2.4×10^5	ND	ND	Fig. S1
P22	M	69	Herpetic iridocyclitis	VZV	3.9×10^8	Positive	—	Fig. S1
P26	F	41	Herpetic iridocyclitis	VZV	1.1×10^6	Positive	—	Fig. S1
P27	M	28	ARN	VZV	4.1×10^5	Positive	—	Fig. S1
P29	M	49	Herpetic iridocyclitis	VZV	3.2×10^5	Positive	—	Fig. S1
P30	F	43	Herpetic iridocyclitis	VZV	3.5×10^5	Positive	—	Fig. S1
P31	F	81	ARN	VZV	3.9×10^6	Positive	—	Fig. S1
U14	F	69	EBV-positive uveitis	EBV	Unmeasured	Positive	—	Fig. S1

ARN, acute retinal necrosis; ND, not detected.

Table 3. Clinical Characteristics of Patients With mPCR-Negative Uveitis

Characteristic	mPCR-Negative Uveitis ($n = 23$)
Age (y), mean ± SD	56.3 ± 14.8
Sex, *n* (%)	
Male	15 (65.2)
Female	8 (34.8)
Type of uveitis, *n* (%)	
Panuveitis	12 (52.2)
Anterior	11 (47.8)
Intermediate	—
Posterior	—

Ethics Statement and Data Availability

Our study was conducted in accordance with the tenets of the Declaration of Helsinki. Institution Review Board (IRB) approval was obtained from the IRB of Nagoya University Graduate School of Medicine (2020-0598). The study was registered with the University Hospital Medical Information Network (UMIN000044906). Written informed consent was obtained from all of the patients.

Sample Collection

This study included 43 patients with anterior uveitis, posterior uveitis, or panuveitis. Among them, 20 tested positive and 23 tested negative for intraocular herpes virus infection, including herpes simplex virus 1 (HSV1), HSV2, varicella zoster virus (VZV), Epstein–Barr virus (EBV), and cytomegalovirus (CMV), as determined by mPCR of aqueous humor samples (Tables 1–3). Patients were excluded if they had intraocular inflammation other than those listed above, such as postprocedural endophthalmitis or noninfectious uveitis (e.g., sarcoidosis, Vogt–Koyanagi–Harada disease, Behçet disease). All samples were collected between April 2017 and January 2023 and stored at −80°C before being used for long-read sequencing analysis. The pathogenicity of EBV for uveitis remains controversial; however, in our study, one sample (U14), which tested positive using mPCR, was included as an mPCR-positive sample.

DNA Purification and Nanopore Long-Read Sequencing Protocol

We used the QIAamp MinElute Virus Spin Kit (QIAGEN, Hilden, Germany) to extract and purify viral genomic DNA from 10 to 20 µL of the collected aqueous humor samples, following the manufacturer's protocol. To obtain a sufficient amount of DNA for analysis, we conducted whole-genome amplification using the REPLI-g UltraFast Mini Kit (QIAGEN) for a variable time ranging from 90 minutes to 24 hours, depending on the variation in viral DNA copy numbers among samples. We quantified the DNA using a Qubit dsDNA Quantification Assay Kit (Q32850; Thermo Fisher Scientific, Waltham, MA, USA) on the Qubit 4.0 Fluorometer (Q33238; Thermo Fisher Scientific). Total genomic DNA, including host DNA, viral DNA, and contaminants, was subsequently treated with transposase, and a sequencing adapter was added using the Rapid Sequencing Kit (SQK-RAD004; Oxford Nanopore Technologies). We assessed DNA quality and fragment size (PCR products and MinION libraries) using the TapeStation 4150 (G2992AA; Agilent Technologies, Santa Clara, CA, USA), an automated electrophoresis platform, with Agilent Genomic DNA ScreenTape (5067-5365) and an Agilent DNA ladder (5067-5366, 200 to >60,000 bp).

We performed long-read sequencing using an Oxford Nanopore Technologies Flongle flow cell (FLO-FLG001 R9.4.1) or MinION flow cell (FLO-MIN106D R9.4.1) measurement chip and generated FASTQ files using MinKNOW 22.05.5 software (Oxford Nanopore Technologies). The input DNA concentration was maintained at 200 ng per

Investigative Ophthalmology & Visual Science

3.75 µL (approximately 53.3 µg/mL) for the Flongle flow cell and 400 ng per 7.5 µL (approximately 53.3 µg/mL) for the MinION flow cell, following the official protocol. The Flongle flow cell and MinION flow cell were used for individual samples (one library), with run times of 72 hours for the MinION flow cell and 24 hours for the Flongle flow cell. To identify the etiologic microorganisms present in the sample, we used the Metagenomic Classification Tutorial algorithm of EPI2ME Labs (Oxford Nanopore Technologies) for pathogen detection, implemented using a Jupyter notebook. To evaluate the phylogenetic composition of microorganisms in the specimen, we displayed all microorganisms except the human genome on the phylogenetic tree using Pavian software.[23] Further downstream analysis for genome coverage was performed using minimap2 with default parameters for long-read data (-a -x map-ont). To evaluate the specificity of detected sequence of the DNA fragments, a BLAST search with default settings was used.[24] Throughout the experiment, we adhered to contamination-avoidance protocols, including the use of laminar flow cabinets, frequent disinfection, and sterile techniques.

Statistical Analysis

To analyze between-group differences, the Kruskal–Wallis test or Fisher's exact test was used. Spearman's rank correlation coefficient was utilized to evaluate the correlation. $P < 0.05$ was considered statistically significant. All statistical analyses were performed using R 3.4.4 (R Foundation for Statistical Computing, Vienna, Austria). We normalized the values of total read counts using the log_scale function in R.

Results

Detection of Etiologic Virus DNA Fragments in Herpetic Uveitis Through Comprehensive Nanopore Metagenomic Analysis

We initially conducted long-read sequencing of 43 aqueous humor samples collected from patients with anterior uveitis, posterior uveitis, or panuveitis and pre-screened using mPCR for intraocular herpes virus (HSV1, HSV2, VZV, EBV, CMV) infection (Tables 2, 3). The metagenomic long-read sequencing was performed using the Flongle flow cell on the MinION platform. The sequencing output-related parameters, including the total generated reads, the total sequencing time required for virus detection (i.e., the shortest time for detecting DNA sequences), the number of reads mapped to the virus genome, their proportion, REPLI-g incubation periods,

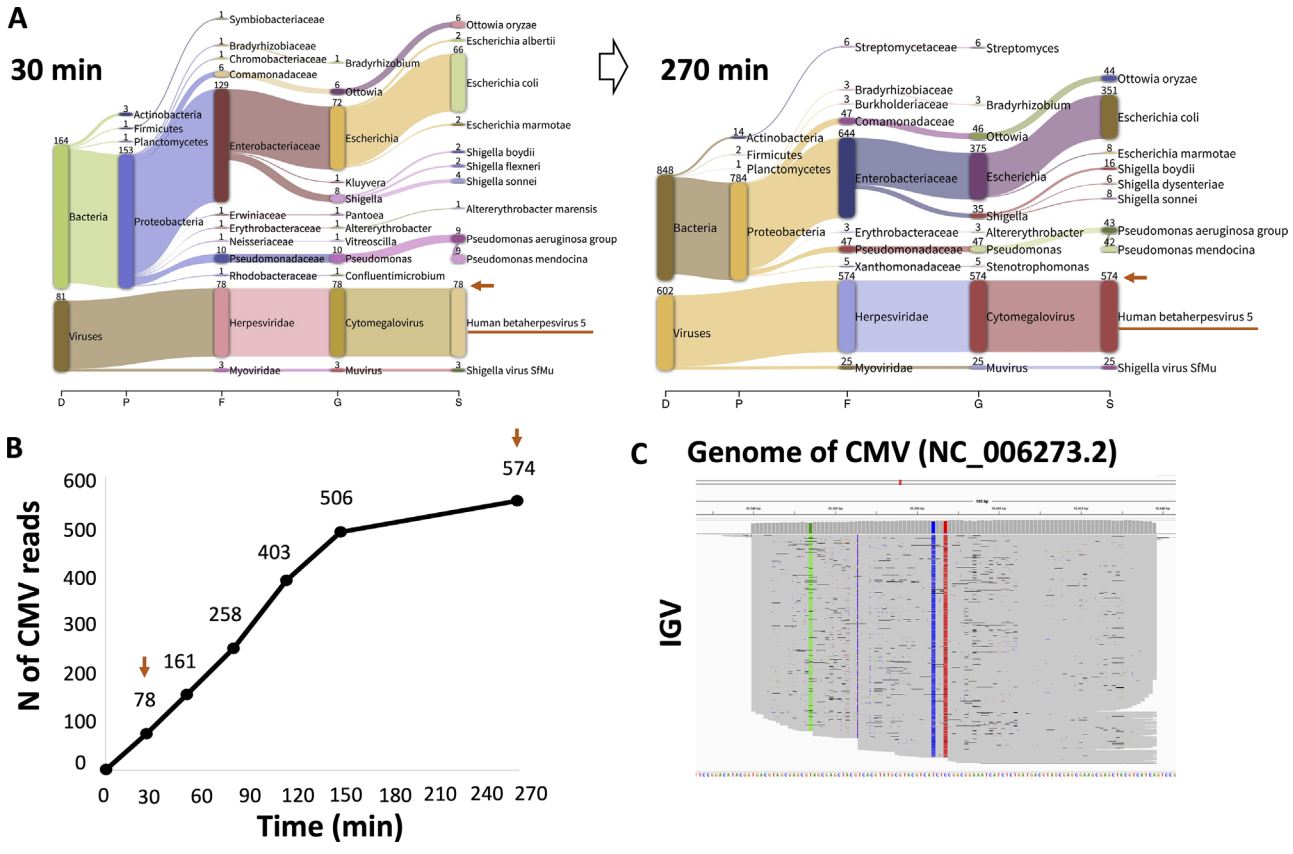

Figure 1. Phylogenetic classification of a representative mPCR-positive uveitis specimen (P5), time-point analysis of the number of sequence reads, and visualization of genomic data. (**A**) Analysis results of case with CMV retinitis (P5), a representative of herpes virus uveitis. The phylogenetic tree (Pavian plot) shows all microorganisms, except the human genome, and quantifies them from *left* to *right* in the following order: domain (D), phylum (P), class (C), family (F), genus (G), and species (S). (**B**) Time-point analysis of the number of sequence reads mapped to the CMV reference genome. The horizontal axis indicates time (minutes), and the vertical axis indicates the number of sequence reads mapped to the reference genome of CMV. CMV DNA reads were detected approximately 30 minutes after sequencing initiation. (**C**) The reads of virus-derived DNA fragments were mapped onto the CMV reference genome and visualized with Integrative Genomics Viewer (IGV). Panel **C** was created using data at the end of the run in Flongle sequencing (i.e., at 24 hours).

Investigative Ophthalmology & Visual Science

sequencing run quality control (mean read quality), and output data volume for each sample are presented in Supplementary Table S1. Among them, 20 samples were detected with a virus, which included VZV, EBV, and CMV (Table 2). We detected DNA fragments of CMV as early as about 30 minutes after sequencing began, at which point diagnosis was considered possible (Figs. 1A, 1B). The tools also produced visualizations of the results of phylogenetic analysis (Fig. 1A, Supplementary Fig. S1).[23]

We mapped and visualized the reads of the detected virus-derived DNA fragments onto the CMV reference genome (Fig. 1C).[24–27] The nanopore metagenomic analysis (NMA) detected the etiologic virus in 60.0% of the 20 mPCR-positive samples (Table 2). Cases in which no etiologic virus was detected by NMA exhibited significantly lower copy numbers by mPCR ($P = 0.02$) (Supplementary Fig. S2). The range of viral DNA copies present in the original specimens of the herpes-positive group, as measured by mPCR, was between 4.2×10^3 and 3.9×10^8 (Supplementary Fig. S2). When comparing the copy numbers of virus DNA in the herpes-positive group and the herpes-not-detected group of uveitis patients, as determined by NMA using the Flongle flow cell, a median copy number of the viral pathogen was approximately 100-fold higher in the former (Supplementary Fig. S2). We compared the output data volume (MB) and normalized total read counts among the herpes-positive and herpes-not-detected groups of uveitis patients as determined by nanopore metagenomic analysis using the Flongle flow cell and found no statistically significant differences between the two groups ($P = 0.41$ and $P = 0.24$, respectively) (Supplementary Fig. S3). In the uveitis cases that tested negative by mPCR (23 cases), nanopore analysis also displayed compatible results in all cases, suggesting high specificity of NMA. Simultaneously, numerous other microorganisms were detected through NMA (Fig. 1A; Supplementary Figs. S1, S4). However, it was assumed that most of them were due to environmental and host contamination, as they were also detected in the metagenomic analysis of sterile saline solution processed in an identical manner (Supplementary Fig. S5).[28]

We performed supplementary analyses to explore the relationships between the REPLI-g amplification period and relative abundance of viral reads, the REPLI-g amplification period and normalized read counts, the normalized viral read counts and log copies of virus DNA measured by mPCR, and the fractional abundance of viral reads and log copies of virus DNA measured by mPCR; however, no statistically significant results were obtained ($P = 0.96$, $P = 0.12$, $P = 0.13$, and $P = 0.39$, respectively) (Supplementary Fig. S6).

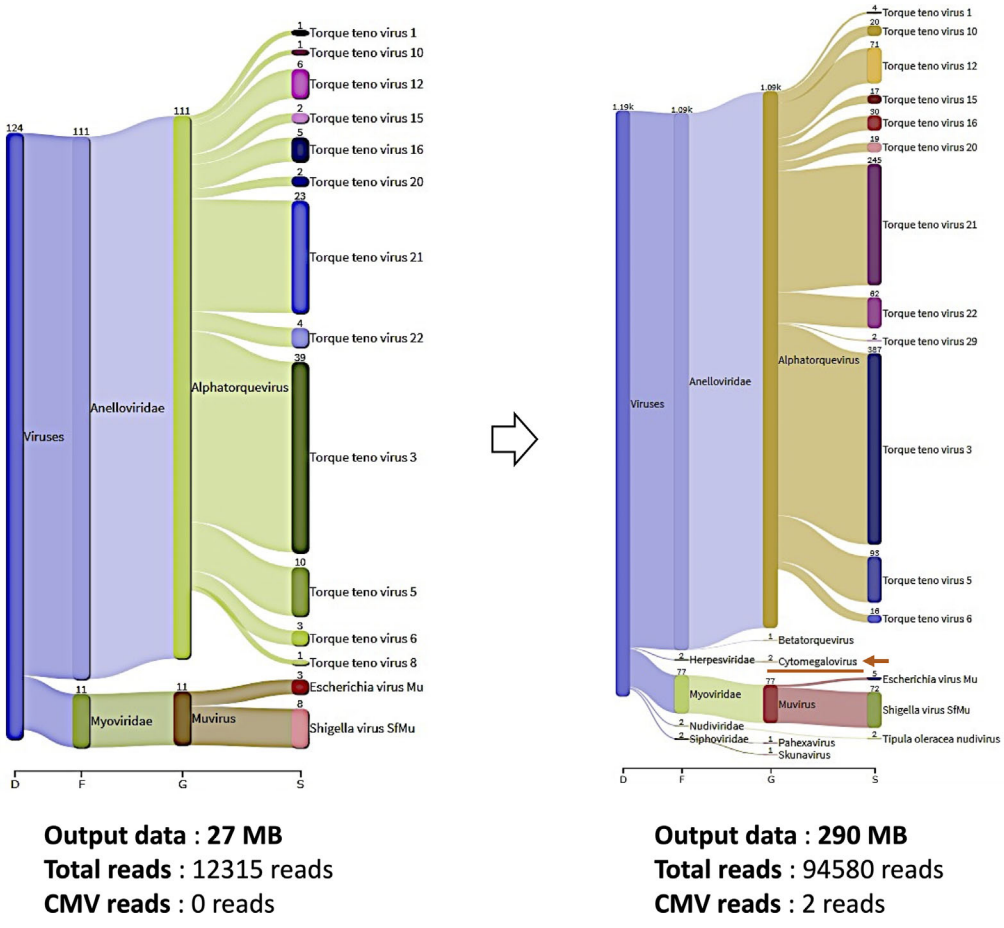

Figure 2. Comparison of Flongle flow cell and MinION flow cell nanopore metagenomic analyses of an mPCR-positive uveitis specimen (P11). To determine the reason for the low sensitivity of the nanopore metagenomic analysis, we used a MinION flow cell to test whether the amount of sequence data affected detection sensitivity in mPCR-positive cases that were negative with Flongle flow cell sequencing. The MinION flow cell produced around 10 times more sequence data than the Flongle flow cell, and two CMV reads were detected.

Investigative Ophthalmology & Visual Science

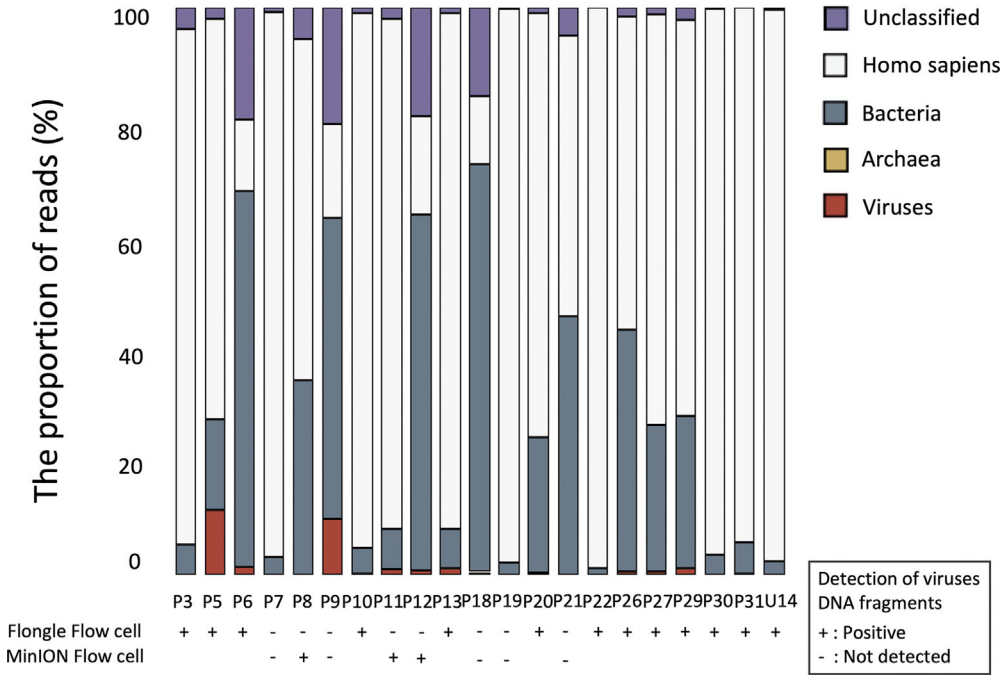

Figure 3. Proportions of *Homo sapiens*, bacterial, archaeal, and viral reads in the output data of nanopore metagenomic analyses of mPCR-positive uveitis specimen. From the 20 specimens positive for the herpes virus with mPCR, we examined the nanopore sequence data origin ratios. In addition to bacteria, viruses, and archaea, the human genome and unclassified nanopore sequence reads were also detected. Samples in which the etiologic virus was detected in the Flongle flow cell or the MinION flow cell are identified by a *plus sign* (+) in the figure, and samples in which it was not detected are marked in the bottom row with a *minus sign* (−).

Improved Sensitivity by Increasing Data Acquisition Using the MinION Flow Cell

Next, we conducted further tests using the MinION flow cell with a greater capacity to process sequencing results on cases that tested negative with the Flongle flow cell. Results indicated that the amount of sequence data produced by the MinION flow cell (mean ± SE, 207432.8 ± 56681.2 reads) was approximately 10 times greater than that produced by the Flongle flow cell (mean ± SE, 15339.0 ± 4642.1 reads). Three cases (P9, P11, and P12) were positive for CMV using the MinION flow cell (Table 2, Fig. 2, Supplementary Fig. S4). Therefore, the MinION flow cell led to virus detection in three of eight cases missed by the Flongle flow cell sequencing. Consequently, the sensitivity increased to 76.2% by combining the results of two types of flow cells (Table 2, Fig. 2, Supplementary Fig. S4). Among the newly solved cases, only two CMV reads were detected in P11 (Fig. 2) by the MinION flow cell, suggesting that the low sensitivity of the nanopore may have been due to an insufficient volume of sequencing data volume in relation to the number of copies of the virus in the specimen. We searched the detected mapped sequence of the DNA fragment using a BLAST search with default settings, and 100% of the top 100 hits were for CMV, confirming that the sequence is highly specific for the CMV genome (Supplementary Table S2), even when only a few reads are present.

Proportions of *Homo sapiens*, Bacterial, Archaeal, and Viral Reads in Sequencing Output Data

In the nanopore sequence data, we examined the proportions of the acquired genome reads from different origins. In addition to bacteria, viruses, and archaea, the human genome and unclassified reads were also detected in the nanopore sequences data (Fig. 3). Genetic materials from human and bacterial genomes were most frequently observed, averaging 68.2% and 25.2%, respectively. Because we targeted virus genomes in this study, we determined the ratio of virus genome reads to reads from other genomes. We compared the ratio of total virus genome reads to the numbers of reads from other genomes for the group in which herpes virus reads were detected by Flongle flow cell sequencing and the group in which they were not detected, but no significant finding was noted ($P = 0.70$) (Supplementary Fig. S7).

Analysis of Clinical Parameters and Response to Antiviral Therapy

The clinical parameters at pre- and posttreatment are presented in Table 4. We found that 89.5% of the patients (17/19) were treated with antiviral treatment, and 9/17 patients (52.9%) showed improvement in clinical parameters. A comprehensive comparison analysis of clinical information in the herpes-positive and herpes-not-detected groups of uveitis patients, as determined by NMA, was conducted, but no significant results were observed (Table 1). We also examined the correlations between clinical symptoms and viral load using relative viral lead ratios, correlations between differences in logMAR best-corrected visual acuity (BCVA) and intraocular pressure (IOP), and differences in relative viral lead ratios among responses to treatments or uveitis types; however, no significant differences were found ($P = 0.26$, $P = 0.14$, $P = 0.76$, and $P = 0.52$, respectively).

Table 4. Clinical Findings and Response to Antiviral Therapy

							Pre-Treatment Clinical Findings						Post-treatment clinical findings						
ID	Gender	Age (y)	Disease	History of Antiviral Treatment?	Types of Antivirals	Treatment Period (d)	BCVA (logMAR)	IOP (mm Hg/ NCT)	Cells in Anterior Chamber	Cells in Vitreous	Vitreous Opacity	Macular Edema	BCVA (logMAR)	IOP (mm Hg/ NCT)	Cells in Anterior Chamber	Cells in Vitreous	Vitreous Opacity	Macular Edema	Response to Antiviral Treatment
P05	Male	61	CMV retinitis	Yes	Valganciclovir, foscarnet	Ongoing	1.00	17	1+	2+	1	+	1.80	7	—	—	0	—	Poor
P06	Female	73	CMV retinitis	Yes	Valganciclovir	257	−0.08	13	1+	1+	1	−	0.10	5	—	—	0	—	Good
P07	Female	63	CMV retinitis	Yes	Ganciclovir	Ongoing	0.22	15	1+	1+	1	+	1.00	16	—	—	—	—	Good
P08	Male	62	Herpetic iridocyclitis	Yes	Valganciclovir	Ongoing	0.52	13	0	0	0	+	1.52	14	0.5+	0	0	+	Poor
P09	Male	66	Herpetic iridocyclitis	Yes	Ganciclovir	140	0.52	19	0	0	0	−	0.15	13	0	0	0	—	Good
P10	Male	59	CMV retinitis	Yes	Ganciclovir, valganciclovir	106	0.52	7	1+	1+	1	−	1.30	7	1	1	1	—	Good
P11	Male	73	CMV retinitis	Yes	Ganciclovir, foscarnet	280	1.40	9	1+	2+	1	+	2.00	6	3	3	1	—	Poor
P12	Female	46	CMV retinitis	Yes	Valganciclovir	432	0.40	17	0	0	0	−	−0.18	15	0	0	0	—	Good
P13	Female	64	CMV retinitis	Yes	Valganciclovir, foscarnet	1212	−0.08	13	1+	1+	0	+	1.00	10	1	1	1	—	Poor
P18	Male	74	Herpetic iridocyclitis	Yes	Valaciclovir	Ongoing	0.22	17	1+	1+	0	−	−0.08	14	1	1	1	—	Good
P19	Female	53	Herpetic iridocyclitis	Yes	Valaciclovir	1402	−0.08	NA	1+	1+	1	−	0.00	23	0	0	0	—	Poor
P20	Male	64	Herpetic iridocyclitis	Yes	Valaciclovir	196	−0.08	16	1+	1+	1	−	0.00	14	0	0	0	—	Good
P21	Male	53	ARN	Yes	Acyclovir, valaciclovir	316	0.00	19	2+	1+	1+	+	0.00	14	0	0	1	—	Poor
P22	Male	69	Herpetic iridocyclitis	Yes	Acyclovir, valaciclovir	85	0.82	15	3	3	1	+	1.15	20	1	0	0	—	Good
P26	Female	41	Herpetic iridocyclitis	No	—	42	−0.18	15	1+	1+	0	−	0.00	15	0	0	0	—	—
P27	Male	28	ARN	Yes	Foscarnet, acyclovir	397	0.40	24	2+	1+	1	+	1.80	6	2+	2+	1	—	Poor
P29	Male	49	Herpetic iridocyclitis	Yes	Valaciclovir	55	0.70	22	2+	2+	1	−	0.00	13	0	0	0	—	Good
P30	Female	43	Herpetic iridocyclitis	No	—	338	0.05	32	1+	1+	0	−	0.00	12	1	1	1	—	—
P31	Female	81	ARN	Yes	Valaciclovir	1009	2.00	21	2+	2+	1	+	0.05	15	1	1	1	—	Poor
U-14	Female	69	EBV-positive uveitis	Yes	Ganciclovir	Ongoing	0.10	12	1+	1+	1	−	2.00	12	1+	1+	0	—	Poor

Discussion

In this retrospective cross-sectional study, we investigated the sensitivity and specificity of herpes virus detection using NMA compared with the mPCR-positive and -negative controls. The results showed that NMA using a Flongle flow cell detected the pathogenic virus in 60.0% of the cases that tested positive by mPCR. The undetected cases had lower viral DNA copy numbers. All viruses detected by NMA were identical to those diagnosed by mPCR, and no samples that were negative by mPCR revealed herpes viral DNA with the use of NMA. Further analysis using the MinION flow cell increased the sensitivity to 75.0%. These results suggest that NMA shows reasonable sensitivity and high specificity for detecting etiologic virus DNA fragments.

We confirmed that increasing the data volume using a MinION flow cell instead of a Flongle flow cell improved the sensitivity of NMA. Our study shows that we were able to detect pathogens in 37.5% of the samples (3/8) where the Flongle flow cell failed to detect pathogens by increasing the amount of data acquired with the MinION flow cell. A Flongle flow cell contains over 50 active pores, whereas a MinION flow cell has more than 800, with each pore reading a single DNA strand at a time for analysis. Three of these samples, including P11, allowed us to detect pathogens with an approximately 10-fold increase in sequencing data (Fig. 2). Considering the fact that the median difference in the number of DNA copies between samples detected by Flongle and those not detected by Flongle was approximately 100-fold in our sample, it is possible that more than 10-fold data volume (approximately 3 GB per sample) is required to achieve sensitivity comparable to that of mPCR (Fig. 2, Supplementary Fig. S2). However, further studies are required to determine exactly how much more data is needed to achieve sensitivity comparable to qPCR test.

The acquisition of comprehensive, hypothesis-free metagenomic information allows for a comprehensive characterization of uveitis by considering all genomic DNA present at the inflammatory site. In this study, the DNA viruses identified by mPCR were also detected by NMA, and there was no other etiologic DNA virus, consistent with these viruses being the only pathogens of uveitis. Although NMA incurs higher running costs than mPCR, even with the relatively inexpensive MinION, adopting the system requires less investment, which may be advantageous in less equipped environments. Actually, this comprehensive method has shown potential application to detect unexpected microorganisms in undiagnosed uveitis apart from proof of their etiology, as we have observed simultaneous infection of herpes virus and torque teno virus (Fig. 2, Supplementary Fig. S1).[29] Furthermore, the high specificity of NMA may play a clinically important role in ruling out DNA virus infection in uveitis cases of unknown etiology.

Another aspect of NMA that requires careful consideration includes the large amount of noise due to bacterial contamination and reagents involved in the whole-genome amplification process, such as phi29 DNA polymerase and the Shigella virus SfMu, which parasitizes *Escherichia coli*, both of which were common anticipated contaminants in this study (Fig. 1A; Supplementary Figs. S1, S4). This has been clearly shown via nanopore analysis of a sterile saline solution that revealed a large number of microorganisms (Supplementary Fig. S5). This background contamination has been pointed out in previous studies.[28,30,31] Various methods were applied to distinguish bacterial pathogens from contamination but with limited success.[17,18] Thus, there is no unified methodology to distinguish contaminating genomes in the metagenomic approach, and this is an issue to address in the future.

This study has several limitations. First, this is a retrospective study, and data collection relies on existing medical records and available stored DNA samples, which may introduce selection bias in the patient population. Second, this study focused only on herpes virus detection using NMA; therefore, generalization of the findings to other types of infections and pathogens may be limited. Third, this study included a relatively smaller sample size, which may also limit the generalizability of the findings. A larger sample size is required to explore the potential benefits of NMA and standardize the widespread adoption of this approach in clinical practice. Fourth, this study did not compare the accuracy of mPCR and NMA. To compare the two methods, the accuracy of NMA should be confirmed using the same controls used in the mPCR accuracy assessment. Fifth, we evaluated only aqueous humor samples. We successfully detected the VZV virus genome in a vitreous sample (P3) using the same method used in this study (Supplementary Fig. S8), which suggests that our method may be useful for vitreous samples. Sixth, with respect to the use of REPLI-g amplification, it was necessary to ensure sufficient input for sequencing; however, this process also increases the host DNA and the inclusion of sequences from contaminating organisms beyond the viral genome. Moreover, the appropriate detection criteria for NMA in viruses have not yet been validated. Seventh, the identified pathogenic microorganisms may not have affected the clinical data. In addition, it was difficult to prove a precise causal relationship regarding the clinical impact of the etiological virus detected by NMA in uveitis in our retrospective study. Finally, this study used retrospectively collected specimens stored for several years, which may have led to some DNA degradation and affected the analysis of long-chain DNA. However, because the primary aim was to confirm the presence or absence of viruses, the impact of DNA degradation is considered minimal. The utility of this method can be enhanced through future evaluations of these aspects.

In conclusion, NMA demonstrated reasonable sensitivity and high specificity for detecting herpes virus DNA fragments in patients with herpetic uveitis. Our study highlights the potential of nanopore sequencing to facilitate further advances in uveitis diagnosis.

Acknowledgments

The authors thank Kazuhiro Horiba, Department of Genetics, Research Institute of Environmental Medicine, Nagoya University, for his advice on library preparation and the use of MinION. The authors wish to acknowledge the Division for Medical Research Engineering, Nagoya University Graduate School of Medicine, for technical support.

This study was presented in part at the 126th Annual Meeting of the Japanese Ophthalmological Society in April 2022 and at the 127th Annual Meeting of the Japanese Ophthalmological Society in April 2023.

Supported by grants from the Japan Society for the Promotion of Science KAKENHI (20K09765 to KMN, 22K16969 to YK, 22K20958 to AFS) and a donation from Sugita Eye Hospital (KY).

Disclosure: **Y. Koyanagi**, None; **A.F. Sajiki**, None; **K. Yuki**, None; **H. Ushida**, None; **K. Kawano,** None; **K. Fujita**, None;

H. Shimizu, None; **D. Okuda**, None; **M. Kosaka**, None; **K. Yamada**, None; **A. Suzumura**, None; **S. Kachi**, None; **H. Kaneko**, None; **H. Komatsu**, None; **Y. Usui**, None; **H. Goto**, None; **K.M. Nishiguchi**, AbbVie (F), Nippon Kayaku (F)

References

1. Sugita S, Takase H, Nakano S. Practical use of multiplex and broad-range PCR in ophthalmology. *Jpn J Ophthalmol*. 2021;65(2):155–168.
2. Sugita S, Ogawa M, Shimizu N, et al. Use of a comprehensive polymerase chain reaction system for diagnosis of ocular infectious diseases. *Ophthalmology*. 2013;120(9):1761–1768.
3. Nakano S, Tomaru Y, Kubota T, et al. Multiplex solid-phase real-time polymerase chain reaction without DNA extraction: a rapid intraoperative diagnosis using microvolumes. *Ophthalmology*. 2021;128(5):729–739.
4. Sonoda KH, Hasegawa E, Namba K, et al. Epidemiology of uveitis in Japan: a 2016 retrospective nationwide survey. *Jpn J Ophthalmol*. 2021;65(2):184–190.
5. Mercanti A, Parolini B, Bonora A, Lequaglie Q, Tomazzoli L. Epidemiology of endogenous uveitis in north-eastern Italy. Analysis of 655 new cases. *Acta Ophthalmol Scand*. 2001;79(1):64–68.
6. Gritz DC, Wong IG. Incidence and prevalence of uveitis in Northern California; the Northern California Epidemiology of Uveitis Study. *Ophthalmology*. 2004;111(3):491–500, discussion 500.
7. Bajwa A, Osmanzada D, Osmanzada S, et al. Epidemiology of uveitis in the mid-Atlantic United States. *Clin Ophthalmol*. 2015;9:889–901.
8. Tsirouki T, Dastiridou A, Symeonidis C, et al. A focus on the epidemiology of uveitis. *Ocul Immunol Inflamm*. 2018;26(1):2–16.
9. Sugita S, Usui Y, Watanabe H, et al. Adenovirus-associated uveitis with necrotizing retinitis. *Ophthalmology*. 2023;130(4):443–445.
10. Kolb AW, Chau VQ, Miller DL, Yannuzzi NA, Brandt CR. Phylogenetic and recombination analysis of clinical vitreous humor-derived Adenovirus isolates reveals discordance between serotype and phylogeny. *Invest Ophthalmol Vis Sci*. 2024;65(2):12.
11. Lewandowski K, Xu Y, Pullan ST, et al. Metagenomic nanopore sequencing of influenza virus direct from clinical respiratory samples. *J Clin Microbiol*. 2019;58(1):e00963–19.
12. Hong NTT, Anh NT, Mai NTH, et al. Performance of metagenomic next-generation sequencing for the diagnosis of viral meningoencephalitis in a resource-limited setting. *Open Forum Infect Dis*. 2020;7(3):ofaa046.
13. Mostafa HH, Fissel JA, Fanelli B, et al. Metagenomic next-generation sequencing of nasopharyngeal specimens collected from confirmed and suspect COVID-19 patients. *mBio*. 2020;11(6):e01969–20.
14. Kasianowicz JJ, Brandin E, Branton D, Deamer DW. Characterization of individual polynucleotide molecules using a membrane channel. *Proc Natl Acad Sci USA*. 1996;93(24):13770–13773.
15. Howorka S, Cheley S, Bayley H. Sequence-specific detection of individual DNA strands using engineered nanopores. *Nat Biotechnol*. 2001;19(7):636–639.
16. Amarasinghe SL, Su S, Dong X, Zappia L, Ritchie ME, Gouil Q. Opportunities and challenges in long-read sequencing data analysis. *Genome Biol*. 2020;21(1):30.
17. Charalampous T, Kay GL, Richardson H, et al. Nanopore metagenomics enables rapid clinical diagnosis of bacterial lower respiratory infection. *Nat Biotechnol*. 2019;37(7):783–792.
18. Low L, Nakamichi K, Akileswaran L, et al. Deep metagenomic sequencing for endophthalmitis pathogen detection using a nanopore platform. *Am J Ophthalmol*. 2022;242:243–251.
19. Ishino M, Omi M, Araki-Sasaki K, et al. Successful identification of *Granulicatella adiacens* in postoperative acute infectious endophthalmitis using a bacterial 16S ribosomal RNA gene-sequencing platform with MinION: a case report. *Am J Ophthalmol Case Rep*. 2022;26(101524):101524.
20. Jun KI, Oh BL, Kim N, Shin JY, Moon J. Microbial diagnosis of endophthalmitis using nanopore amplicon sequencing. *Int J Med Microbiol*. 2021;311(4):151505.
21. Huang Q, Fu A, Wang Y, Zhang J, Zhao W, Cheng Y. Microbiological diagnosis of endophthalmitis using nanopore targeted sequencing. *Clin Experiment Ophthalmol*. 2021;49(9):1060–1068.
22. Li X, Li Z, Wang M, et al. The diagnostic utility of nanopore targeted sequencing in suspected endophthalmitis. *Int Ophthalmol*. 2023;43(8):2653–2668.
23. Breitwieser FP, Salzberg SL. Pavian: interactive analysis of metagenomics data for microbiome studies and pathogen identification. *Bioinformatics*. 2020;36(4):1303–1304.
24. Altschul SF, Gish W, Miller W, Myers EW, Lipman DJ. Basic local alignment search tool. *J Mol Biol*. 1990;215(3):403–410.
25. Robinson JT, Thorvaldsdóttir H, Winckler W, et al. Integrative genomics viewer. *Nat Biotechnol*. 2011;29(1):24–26.
26. O'Leary NA, Wright MW, Brister JR, et al. Reference sequence (RefSeq) database at NCBI: current status, taxonomic expansion, and functional annotation. *Nucleic Acids Res*. 2016;44(D1):D733–D745.
27. Schoch CL, Ciufo S, Domrachev M, et al. NCBI Taxonomy: a comprehensive update on curation, resources and tools. *Database (Oxford)*. 2020;2020:baaa062.
28. Salter SJ, Cox MJ, Turek EM, et al. Reagent and laboratory contamination can critically impact sequence-based microbiome analyses. *BMC Biol*. 2014;12:87.
29. Sajiki AF, Koyanagi Y, Ushida H, et al. Association between torque Teno virus and systemic immunodeficiency in patients with uveitis with a suspected infectious etiology. *Am J Ophthalmol*. 2023;254:80–86.
30. Eisenhofer R, Minich JJ, Marotz C, Cooper A, Knight R, Weyrich LS. Contamination in low microbial biomass microbiome studies: issues and recommendations. *Trends Microbiol*. 2019;27(2):105–117.
31. de Goffau MC, Lager S, Salter SJ, et al. Recognizing the reagent microbiome. *Nat Microbiol*. 2018;3(8):851–853.